The cellular automata inside optical chimera states

Saliya Coulibaly, Marouane Ayyad

▶ **To cite this version:**

Saliya Coulibaly, Marouane Ayyad. The cellular automata inside optical chimera states. Chaos, Solitons & Fractals, 2021, 153, pp.111524. 10.1016/j.chaos.2021.111524 . hal-03553737

HAL Id: hal-03553737
https://hal.science/hal-03553737v1

Submitted on 5 Jan 2024

HAL is a multi-disciplinary open access archive for the deposit and dissemination of scientific research documents, whether they are published or not. The documents may come from teaching and research institutions in France or abroad, or from public or private research centers.

L'archive ouverte pluridisciplinaire **HAL**, est destinée au dépôt et à la diffusion de documents scientifiques de niveau recherche, publiés ou non, émanant des établissements d'enseignement et de recherche français ou étrangers, des laboratoires publics ou privés.

Distributed under a Creative Commons Attribution - NonCommercial 4.0 International License

Version of Record: https://www.sciencedirect.com/science/article/pii/S096007792100878X
Manuscript_17e3f1e7d9672a534a31fea90b793e39

The cellular automata inside optical chimera states

Marouane Ayyad[a], Saliya Coulibaly[a]

[a] *Université de Lille, CNRS, UMR 8523 - PhLAM - Physique des Lasers Atomes et Molécules, Lille, F-59000, France*

Abstract

Cellular automata are conceptual discrete dynamical systems useful in the theory of information. The spatiotemporal patterns that they produce are intimately related to computational mechanics in distributed complex systems. Here, we investigate their physical implementation in the framework of chimera states in which coherent and incoherent behavior coexist. Hence, chimera states were subject to quantitative and qualitative analyzes borrowing the same tools used to characterize cellular automata. Our results reveal the existence of cellular automata-type dynamics submerged in the dynamics exhibited by our optical chimera states. Thus, they share a panoply of attributes in terms of computational abilities.

Keywords: Cellular automata, Chimera states, Coupled oscillators, spatiotemporal chaos

1. Introduction

Spontaneous self-organization and intricate collective behaviors within complex extended systems, have been subject to a central focus of physical, chemical and biological researches [1–3]. An accurate theoretical description of a spatiotemporal motion may result in the accurate modelling of the key ingredients: the energy exchanges and the transport mechanisms. When the system is made of independent subsystems, transports are no more ruled by flux base processes such Fick or Fourier law. With these later phenomena the modellings generally lead to partial differential equations (PDE). However, when the spatial extension results in the juxtaposition of independent systems, the interaction is governed by a coupling operator determined by

Email address: marouane.ayyad@univ-lille.fr (Marouane Ayyad)

© 2021 published by Elsevier. This manuscript is made available under the CC BY NC user license
https://creativecommons.org/licenses/by-nc/4.0/

the topological configuration. The obtained dynamical systems are known as coupled map lattices (CML) [4] that are, discrete equations. In spite of the significant difference between continuous (PDE) and discrete (CML) equations, they exhibit analogue spatiotemporal evolution [5]. The interest in the coupled discrete systems has been renewed after they were demonstrated to support coexisting coherent and incoherent domains [6]. The resulting dynamical objects are known as chimera states [7] and their study is currently a very hot topic in nonlinear dynamics [8–16]. For a decade after the first demonstration, chimera states were meant to emerge only in lattice with non-local and global coupling. However, it is now admitted that local or the nearest neighbor coupling can also support chimera states in both 1D [16] and 2D [17] lattices. In these cases, chimeras are generally pinned domain walls separating spatiotemporal chaotic evolution and regular state. Notice that, now chimera states are not only limited to discrete media since continuous counterparts were also reported in continuous systems [18, 19]. An outstanding feature of chimera state is the diversity of the patterns produced by their dynamics. One specific case have kept our attention. Indeed, chimera observed in locally coupled 1D optical waveguides array, triangular domains were observed [20]. Such an evolution known as Sierpiński patterns are universal [5, 21] nonlinear solution and typical of spatiotemporal intermittency. Sarpinsky patterns are also a typical behavior in another class of discrete systems: the elementary cellular automata.

Cellular automata (CA) are part of the standard models for spatially extended dynamical systems, which stand out from the other models by their space-time discreteness. They were introduced by Wolfram who was interested in the relationship between dynamical systems behavior and their computational abilities [22]. In particular, the complex class **IV** CA which supports emergent localized structures known as **blinkers** and propagating structures named **gliders** (see Fig.1a). Wolfram conjectured that all class **IV** rules were capable of universal computation [22, 23]. It is worth mention that the ability to support computation is conditioned by the reconciliation between three essential features: **information storage**, **information transfer** and **information modification** [24].

Despite all these spatiotemporal complexity properties and information processing abilities, CA mainly remain discrete, abstract computational systems. Indeed, for now very few implementations of CA have been reported in physical systems. The aim of this paper is to study the ability of optical chimera states (OCS) to afford properties of elementary cellular automata

(ECA). To this end, we have implemented a classification of the ECA which helped to cluster them according to their dynamical category. The clustering process is then applied to our OCS, allowing us to identify the ECA property that can inherit the OCS. The paper is organized as follows. After a brief state of art on the ECA, we introduce the clustering method implemented thanks to the approximate entropy, the sample entropy [25] and the Lempel-Ziv complexity [26]. Then we consider the dynamics of the OCS in the light of the clustering process before the concluding remarks.

2. Elementary cellular automata (ECA)

In general, a CA comprise a lattice of N identical cells or sites. The state of each cell i at the step time t is denoted $\mathbf{X}_i^t$. To define properly a CA, one must precise: the dimension d of the arrangement of cells, the number of possible states per cell k from the alphabet S, the number of neighbors connected to the central cell i in each direction, called the radius r and a local transition rule φ playing the role of an equation of motion. According to this latter φ, each cell i is updated to the next state $\mathbf{X}_i^{t+1}$ as a function of its current state $\mathbf{X}_i^t$ and those of its neighbors taken into consideration r. In this paper, we will deal with the elementary cellular automata ECA, proposed by Wolfram [22, 27] which are defined as one dimensional $d = 1$ array of cells, subject to periodic boundaries conditions $\mathbf{X}_i^t = \mathbf{X}_{i+N}^t$, with two possible binary states per site ($k = 2$, $S = \{0, 1\}$), and where the size m of the spatially neighborhood of a cell i is related to the radius $r = 1$, (one cell per each side) with the relation $m = 2r + 1 = 3$. In this case of binary state-CA, the local update function $\varphi(m)$ is known as the rule table (See Table 1 and 2). It enumerates the $k^m = 2^3 = 8$ possible configurations $(\mathbf{X}_{i-r}^t\ \mathbf{X}_i^t\ \mathbf{X}_{i+r}^t)$, that the neighborhood can be in. Then, the next generation is given by:

$$\mathbf{X}_i^{t+1} = \varphi(\mathbf{X}_{i-1}^t, \mathbf{X}_i^t, \mathbf{X}_{i+1}^t). \tag{1}$$

For a given rule and an initial condition, successive updates may produce some particular patterns. Illustrations of this behavior for the example of rule 110 and 18 (arbitrary chosen) are shown in Figs. 1a) and b), respectively. In these space-time diagrams, black cells stand for the state 0, and white cells for 1. These two examples are also the proof that despite their apparent simplicity, ECA show a large variety of dynamic behaviors.

In general, in extended dynamical systems the evolution is ruled by a set of order parameters. Hence, their asymptotic behavior is independent of the

Table 1. Rule table of ECA 110, enumerating the evolution of the 8 possible situations.

Neighborhood	111	110	101	100	011	010	001	000
Next generation for central cell	0	1	1	0	1	1	1	0

Table 2. Rule table of ECA 18, enumerating the evolution of the 8 possible situations.

Neighborhood	111	110	101	100	011	010	001	000
Next generation for central cell	0	0	0	1	0	0	1	0

initial stage. However, for CA the asymptotic state was shown to be related to the initial condition [28], making difficult their classification.

Therefore a great part of the state of art in the study of CA is related to their classification and two main schools of thought of classification emerge. The *phenotypic* classification based on the quantification of observed space-time dynamic [24, 29, 30] and the *genotypic* classification founded on the parametrization of rule tables [24, 31].

The pioneer attempt was proposed by Wolfram to classify the ECA [22]. His heuristic classification is based on investigating the "average" spatio-temporal behavior observed over a sample of random initial configurations.

Wolfram's phenotypic classification remains qualitative. To quantify the behavior of CA, several studies based on statistic properties were reached, either on the space-time diagram [24, 29, 30], or on the rule table [24, 31].

3. Optical chimera states (OCS)

The optical chimera states we consider here were reported in ref. [20]. We considered a one dimensional array of nonlinear wave-guide resonators (WGs) locally coupled, subject to coherent optical injection E_0, whose spatiotemporal dynamic is described theoretically by the discrete Lugiato-Lefever model [32,

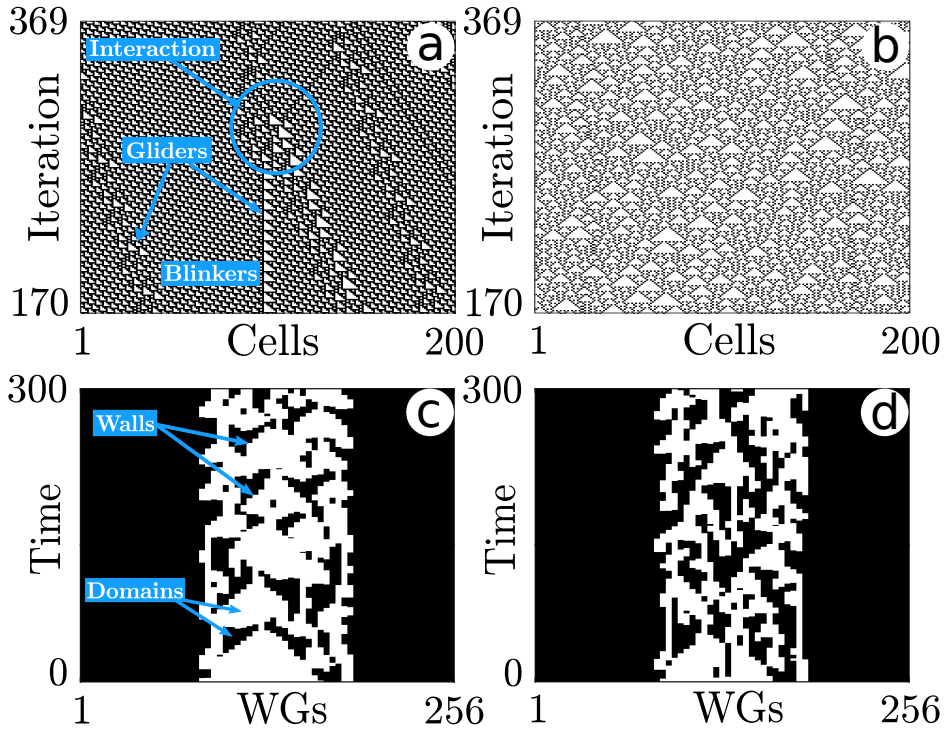

Fig. 1. (Color Online) Illustration of the phenotypic analogy between the emergent patterns showed by OCS and ECA. (a) and (b) space-time diagrams illustrating the typical behavior of complex ECA 110 and chaotic ECA 18, respectively, started from random initial conditions on a 300 cell lattice. (c) and (d) display the filtered spatiotemporal evolutions of the binarized intensity $||\psi_n(t)||^2$ within the desynchronized region of two OCS, obtained from numerical simulations of model Eq. (2) for $C = 1.9$, $\Delta = 7$, $E_0 = 6.2$ (c) and $E_0 = 6.10$ (d).

33]. The intracavity field obeys:

$$\partial_T \psi_n = E_0 - (1 + i\Delta)\psi_n + i|\psi_n|^2\psi_n + iC(\psi_{n+1} - 2\psi_n + \psi_{n-1}), \qquad (2)$$

where ψ_n is the slowly varying envelope of the electric field circulating in the nth micro-resonator, $\Delta \equiv \omega - \omega_0$ stands for the detuning between the resonance frequency ω_0 of the cavity and the input frequency ω, and C stands for the coupling parameter. The evolution time $t = T\tau_{ph}$ is measured in the photon lifetime unit τ_{ph} (is normalized to the cavity decay time).

The Eq. (2) is known to support chimera states as reported in [20, 34]. A typical evolution of such a chimera is displayed in Fig. 2a, obtained following the results reported in [20]. After a binarization process described in Ap-

pendix B, we obtain the evolution of Fig. 2b. Figures 1c) and d) were also obtained by the same method. It should be noted that those OCS demonstrate robustness, flexibility and scalability of their spatiotemporal patterns. Indeed, by the simple modification of the input parameters, one can favor the generation of a wide range of geometrical structures in space-time, leading to more complexity.

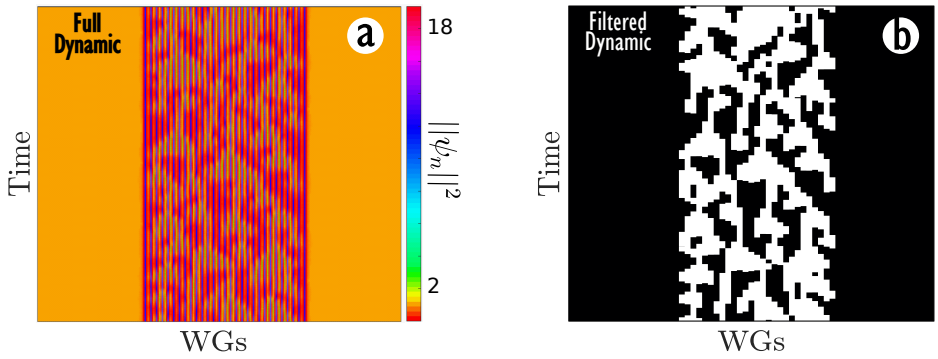

Fig. 2. (Color Online) Optical chimeras states. (a): Spatiotemporal evolution of the intensity $||\psi_n(t)||^2$, obtained from numerical simulations of model Eq. (2) by taking $C = 1.9$, $\Delta = 7$ and $E_0 = 6.15$. (b): the filtered version of (a), displaying the cellular automata dynamic-type submerged.

Hence, the spatiotemporal dynamics showed by our OCS display many of the basic ingredients required to perform the information processing, from the point of view of the computation theory. For instance, the domains, embedded particles (walls between domains) and particle collisions shown in Figs. 1c) and d). Given that experimental implementations of CA are rather few in number, the proposed setup is an opportunity to investigate the CA in the context of nonlinear optics.

To this end, we will first perform a classification of the ECA according to the dynamics they can display. Then, the same process will be applied on the OCS to determine to which class of ECA they belong. CA can be considered following two approaches: the computational mechanics framework [35–38] or analysis will be based on the statistical approach [24, 29, 30]. Here, we will prefer the latter approach.

4. Quantitative overview of ECA and OCS Dynamics

Ordered and random behaviors are simple to be discerned either visually or described statistically [39]. Nonetheless, complex behavior and patterns are easy to identify qualitatively but their quantification remains a nagging puzzle [40]. As mentioned earlier, recognizing the fundamental role of the emergent and interacting structures has driven a panoply of statistical surveys to address this quantification issue, attempting to define a relative location where physical systems with complex behavior lie [24, 30, 38, 40–42]. It is in the light of these statistical tools that we will lead a quantitative analysis of the spatiotemporal dynamics exhibited by ECA and OCS. However, we will focus our efforts in the finding of quantities that allows to classify the ECA according to their dynamical evolution.

First, we classify the different types of dynamics in ECA, in particular, to screen out the complex class. Then, we extend the study to OCS dynamics, seeking to which ECA class, it could be compared, and finally allowing us to build the bedrock of the promising analogy proposed throughout this paper. The concept of entropy to quantify the amount of information loss and to measure the degree of randomness and unpredictability within a dynamical process will be our key tool. Indeed, we adopt Lempel-Ziv complexity (LZ) [26, 43], Approximate entropy (ApEn) [44], and Sample entropy (SampEn) [45]. These three quantities, have different theoretical aspects, but all of them have their roots in information theory and chaos theory. Also, they present a commonplace in the analysis of the discrete series.

It must be pointed out that these three deterministic quantities are maximized for random process and vanish for perfectly ordered ones. Details about these concepts and their implementation can be found in [25, 26, 43–45] and references therein. Inspired by the body of the literature dealing with the characterization of the complexity within experimental signals, using a single observable [25, 46, 47], our study will be based on a time series analysis. The outlines of our method are described in Appendix Appendix B.

5. Results and discussion

5.1. The clustering classification method

For the classification of the ECA we use the clustering strategy. Hence, for each ECA we have computed the ApEn, the LZ complexity and the

SampEn for hundred of different random initial conditions. In Fig. 3a) and b), we have represented these entropies in the plane (LZ, ApEn) and (LZ, SampEn), respectively. As can be seen from these figures, we have various clusters in the entropy planes.

Notice that we recover classifications previously proposed in [22, 31, 48]. Periodic rules class represents the ordered region (orange dots cloud), having low entropy values, while chaotic rules class with high values of entropy, represents the disordered region (black dots cloud). As expected, rules class with complex behavior (gray dots cloud), characterized by an intermediate entropy, are likely to be found in the critical region, located between the ordered and disordered regions. We have also represented the three entropies, for each ECA rule and all the random initial conditions in Figs. 3c), d), and e). Remarkably, we observe from these figures an interesting correlation regarding the randomness values calculated from the behavior of a given ECA rule and its equivalents, over the sample of random initial conditions, such as complex rules: 54 and 147 or rule 110 and 124, 137, 193.

Next, we have extended our analysis to OCS dynamics. The results are given by the triangles in Figs. 3a) and b). It can be seen that they belong to the cloud of complex class (gray dots cloud). This shows that our methodology captures and quantifies neatly the complex behavior and also confirms that this latter lies to the transition from regular towards chaotic phase.

Piecing the above results together, we can conclude that OCS can be classified in the complex behavior class of ECA. This class plays a central role in the hypothesis of "edge of chaos" (EOC) [24, 40, 49, 50], which in turn is a key concept in the information theory. Indeed, systems in such critical regime enhance their computational abilities. The statistical rationale behind this conjecture is that **information storage** requires low entropy (order), while **information transmission** necessitates high entropy (disorder), thus the EOC regime may afford the optimal trade-off [24].

To test the robustness of our results, calculations were performed for different network sizes (N) of ECA in Fig. 4 and various time steps (length of time series L) in Fig. 5, showing no change in our results. Furthermore, our technique shows the potential to classify spatiotemporal configurations, for a spectrum of ordered, complex and chaotic dynamics, without splitting the space and time analysis, thanks to the compression of spatial information in a time series observable such as the mean value.

Now, let's consider the capacity of the system to carry out a useful computational task [37]. In this context, the equation of motion which governs

the system is seen as the program/algorithm, the initial condition as the input and the desirable configuration as the output. Furthermore, the ability of a system to perform universal computation, implies that it should be capable to bear information by reflecting perturbations made to the input and to transmit it to the output [51, 52]. In other words, a universal system must show its sensitivity to external stimulus. For instance, Wolfram speculated that complex ECA class is capable of universal computation, due to the undecidability concerning its behavior [22, 23]. In our survey, this undecidability is mirrored by the large interval values of statistical measures taken by the complex ECA (See e.g. Fig. 3). Notice that, the unpredictability of our OCS dynamics regarding the initial conditions, was demonstrated by computing the Lyapunov exponents [20]. Therefore, the OCS can be seen as a complex dynamical system with properties of the ECA.

An interesting feature of the OCS is that their properties can be controlled by the set of pertinent parameters of the system. An illustration of this feature can be observed in Fig. 6. In this figure, we show in the plane (LZ, ApEn) the entropies of the complex class ECA and the OCS for different values of the pump parameters E_0 (colored markers in Fig. 6a)) and different values of the detuning Δ (colored markers in Fig. 6b)). The color map in both figures accounts for the change of the size of the OCS's incoherent domain δ_L. It appears that the properties of the ECA inherited by the OCS can be continuously tuned by almost all the parameters of the system and also the profile of the chimera. Therefore, with our clustering method, we are able to quantify the qualitative change between the different types of spatiotemporal evolution as the parameters change (see space-time diagrams in inset of Fig. 6).

To complete our analogy, we have deepen the study to compare the properties of our OCS and those of ECA complex rules. We consider the long term dynamics. Various authors [24, 53] have reported that in the vicinity of the phase transition, ECA can exhibit long transients which are function of the array size. Consequently, one can expected that the entropies to be also function of the size. This is what we observed in Fig. 7a), where we have plotted the average of the entropy value estimated by ApEn over 100 random initial configurations as a function of array size N for ECA complex rules 110 (blue) and 54 (green). In contrast to the rule 54, which remains less complex, the rule 110 dynamic shows a sensitivity to size, through the growth tendency of ApEn with system size. This scaling behavior of rule 110, can be explained as a direct consequence of its transient time, which in-

creases with system size [53]. Here also, we observe the same behavior with our OCS as can be seen with Fig. 7b) where we show the ApEn as function of the chimera size δ_L.

It must be pointed that this extended tendency of complexity has been qualified fundamental to support information processing [24, 54].

Another property suggested to have relationship with computational universality is the $1/f^{\alpha}$ noise property of the spectrum. Hence, to explore more horizons concerning the analogy between our OCS and ECA complex rules, we have performed spectral analysis to investigate the temporal behavior. Indeed, a classification of ECA based on the shape of their power spectra were proposed in [54]. Interestingly, the power spectrum $S(f)$ of complex ECA rules (e.g. 110 and 54), exhibit a power law at low frequencies [54] as illustrated in Fig. 8a) and b). Calculations were performed from evolutions starting from a random initial configuration of 3000 cells for 5000 time steps. This spectral decay, known as $1/f^{\alpha}noise$ [55], reflects the strong influence of past events on the future. Ninagawa founded that only rule 110 exhibits $1/f^{\alpha}noise$ during the longest time steps, thanks to its extended transient behavior [53]. Ninagawa claimed that the transient behavior generates intermittency and causes $1/f^{\alpha}noise$ (The bursts and periodic phases, produced by the collision or not of **gliders**). Hence, based on the fact that intermittency represents one of the main mechanisms leading to $1/f^{\alpha}noise$, in chaotic dynamical system [56], our intermittent OCS [20] stem their legitimacy to show a power spectrum whose shape resembles more to the one exhibited by the ECA 110 as it can be seen in Fig. 8b) and c), respectively. Most notably, the presence of $1/f^{\alpha}fluctuation$ in two computationally universal CA, such as ECA 110 [57] and the game of Life [58], has led Ninagawa to conjecture a relationship between computational universality and $1/f^{\alpha}noise$ in CA [59].

6. Conclusion

In conclusion, chimera states are dynamical structures with intriguing feature to support coexistence of coherent and incoherent domains in an array of identical oscillators. They are universal objects that have been observed in a large variety of dynamical systems. In this work, we have considered chimera states exhibited by an array of optical wave-guides locally coupled. We have studied the ability of the optical chimera states to mimic the dynamics of cellular automata, which have many application in computational mechanics. To this end, we have in a first time, classify the cellular automata using a

clustering method based on three metrics: the Approximate, the Sample and the Lempel-Ziv entropies. Hence, the optical chimera states can be cast in this map to identify from which class of cellular automata they inherit their properties and the kind of computation they can perform. To the best of our knowledge, this is one of the first study suggesting that chimera state can afford properties of computational object. This opens the possibility of physical implementation of cellular automata, with promising applications in many domains. Indeed, we are currently in the process of investigating those computational performances in the framework of recurrent neural networks.

Acknowledgements

SC, and MA acknowledge the LABEX CEMPI (ANR-11-LABX-0007) as well as the Ministry of Higher Education and Research, Hauts de France council and European Regional Development Fund (ERDF) through the Contract de Projets Etat-Region (CPER Photonics for Society P4S).

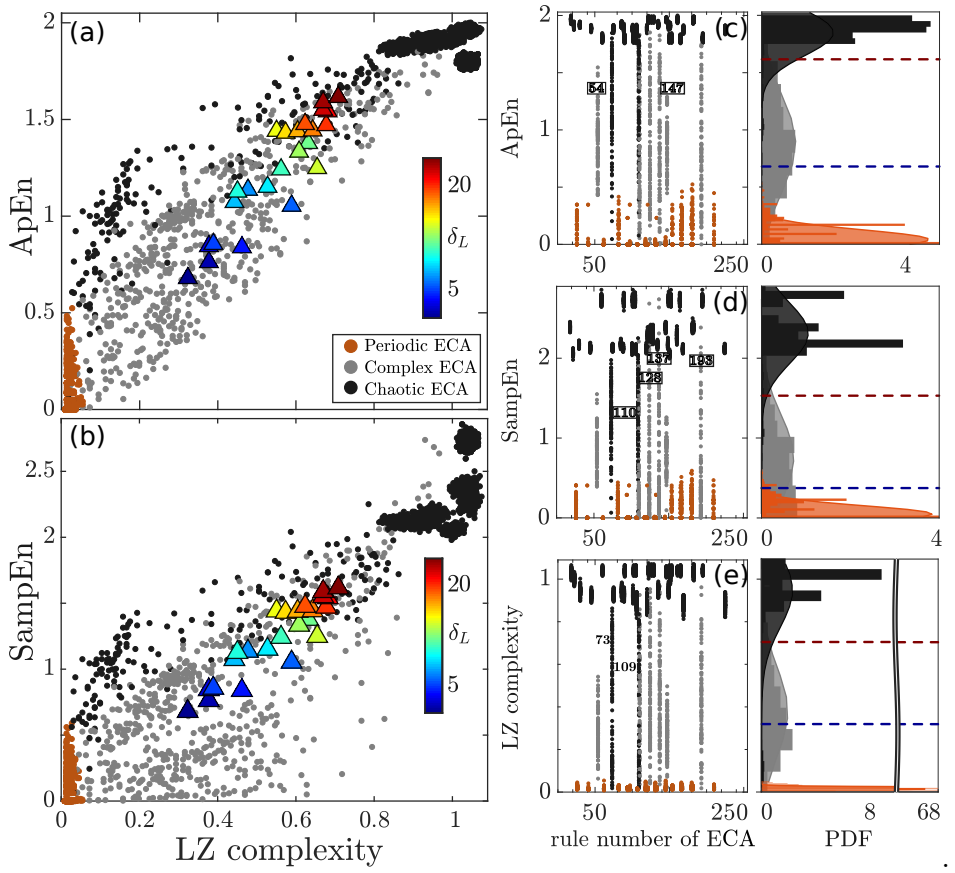

Fig. 3. (Color Online) "Edge of chaos": Statistical overview of the spatiotemporal dynamics of OCS and ECA. (a) and (b) correspond to the maps of ApEn vs LZ and SampEn vs LZ, respectively. Dots correspond to ECA and triangles to OCS. Triangles are obtained for different sizes δ_L of OCS, with $C = 1.9$, $\Delta = 7$ and $E_0 = 6.05$. The left panels show on the three statistical quantities with their frequency histograms (PDF): ApEn (c), SampEn (d) and LZ complexity (e), for all the ECA rules. The minimum (blue) and the maximum (red) values of OCS are illustrated as dashed lines.

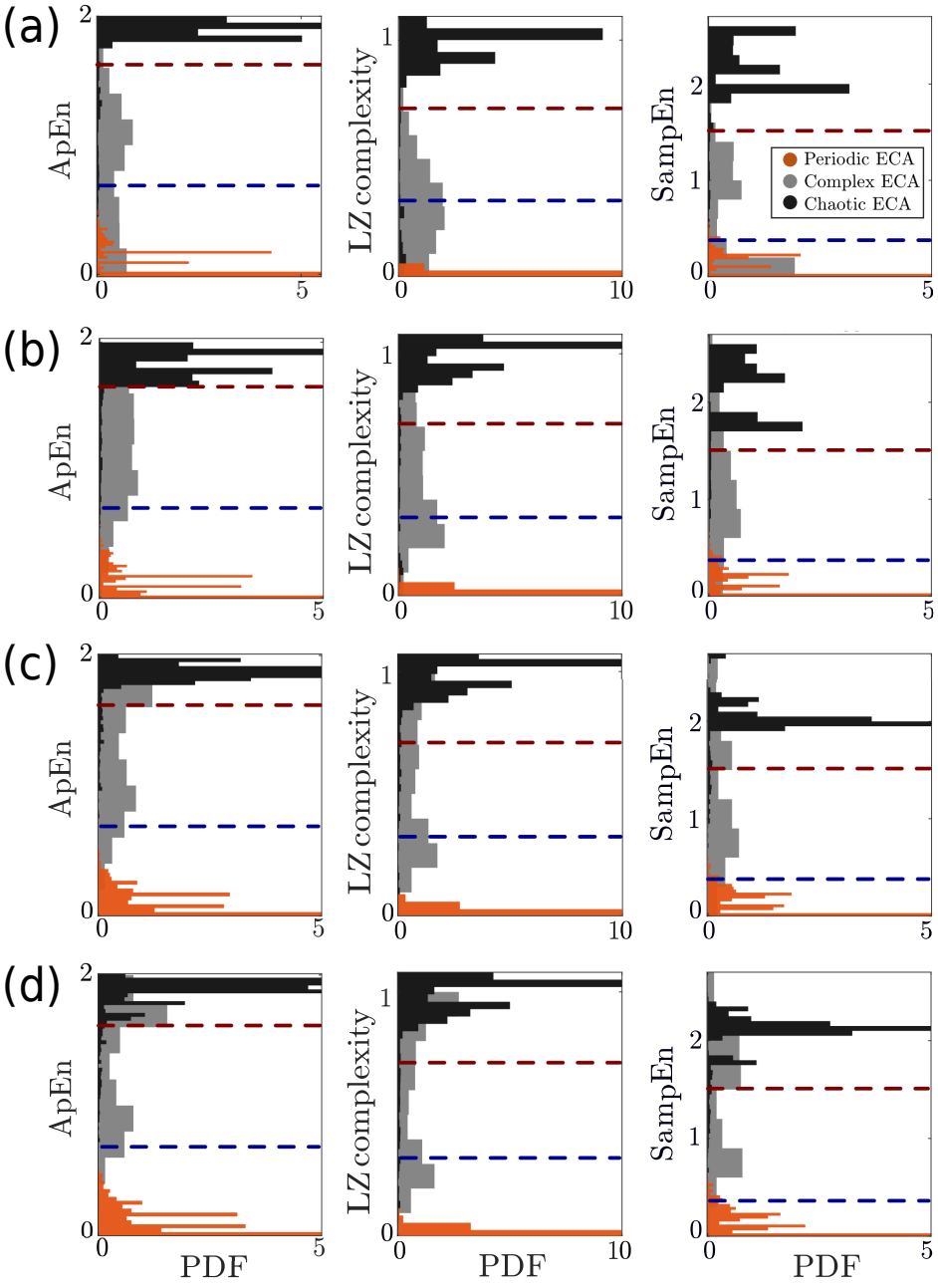

SF. 4. (Color Online) Robustness of results: different network sizes of ECA. (a): $N = 200$, (b): $N = 400$, (c): $N = 600$, (d): $N = 800$. The minimum (blue) and the maximum (red) values of OCS are illustrated as dashed lines (data from Fig. 3).

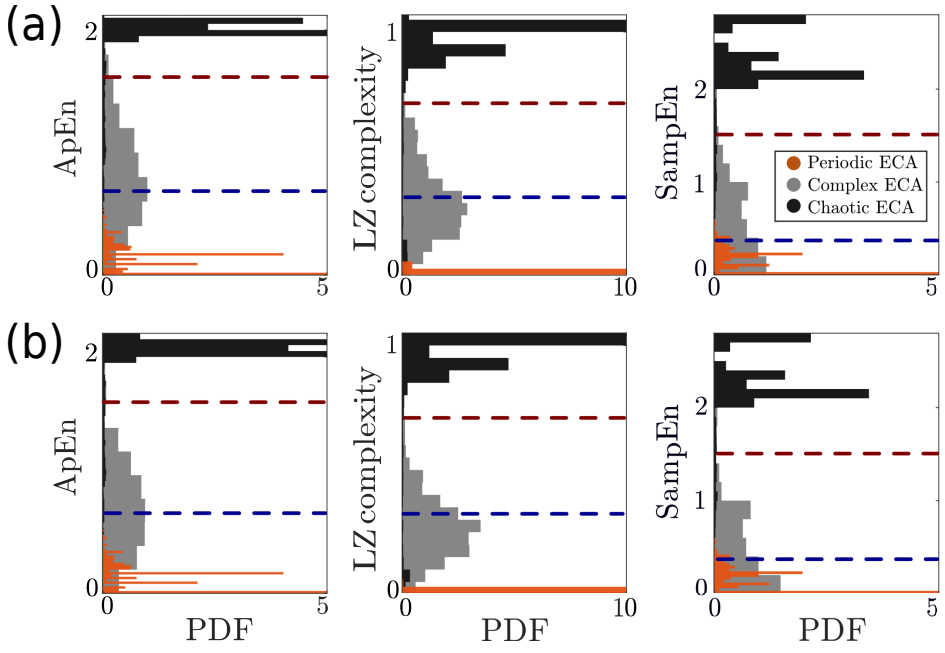

SF. 5. (Color Online) Robustness of results: different lengths of time series(L) for $N = 300$ ECA network size. (a): $L = 3500$, (b): $L = 4500$. The minimum (blue) and the maximum (red) values of OCS are illustrated as dashed lines (data from Fig. 3).

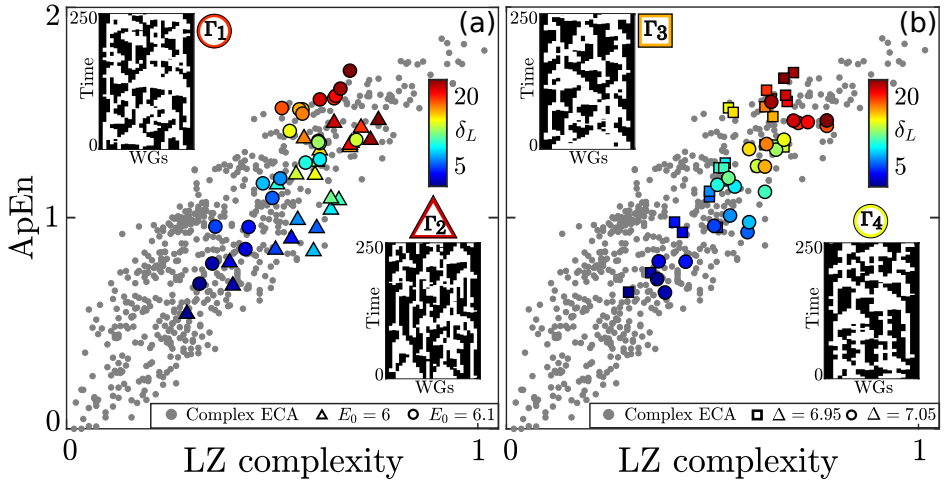

Fig. 6. (Color Online) Sensitivity of ECA and OCS to the driving. Two maps: ApEn against LZ complexity(data from Fig. 3) displaying only the cloud of ECA complex class (gray) and the different OCS sizes δ_L generated with different input parameters (triangle, square and circle markers). (a): $C = 1.9$, $\Delta = 7$ and different $E_0 = 6, 6.1$; (b): $C = 1.9$, $E_0 = 6.05$ and different $\Delta = 6.95, 7.05$. Γ_1 ($\delta_L = 20$), Γ_2 ($\delta_L = 22$), Γ_3 ($\delta_L = 17$) and Γ_4 ($\delta_L = 15$) are selected dynamical evolution to illustrate the configurablity of OCS.

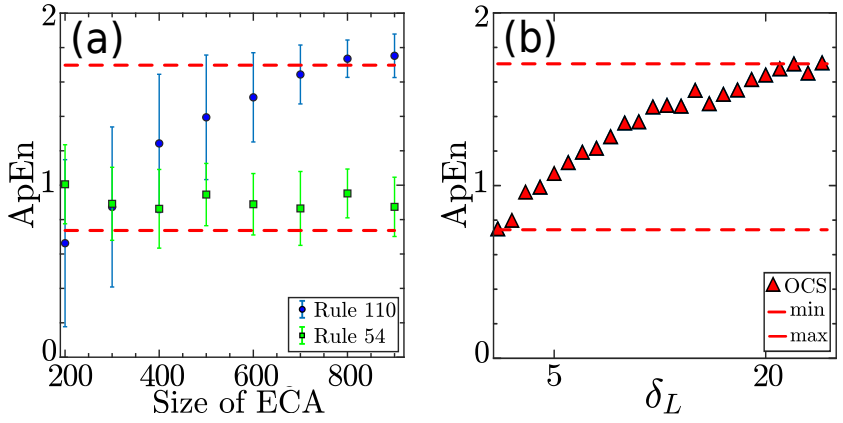

Fig. 7. (Color Online) Scaling behavior of complex ECA rules and OCS: (a) and (b) represent the size effect on ApEn of complex ECA and OCS, respectively.

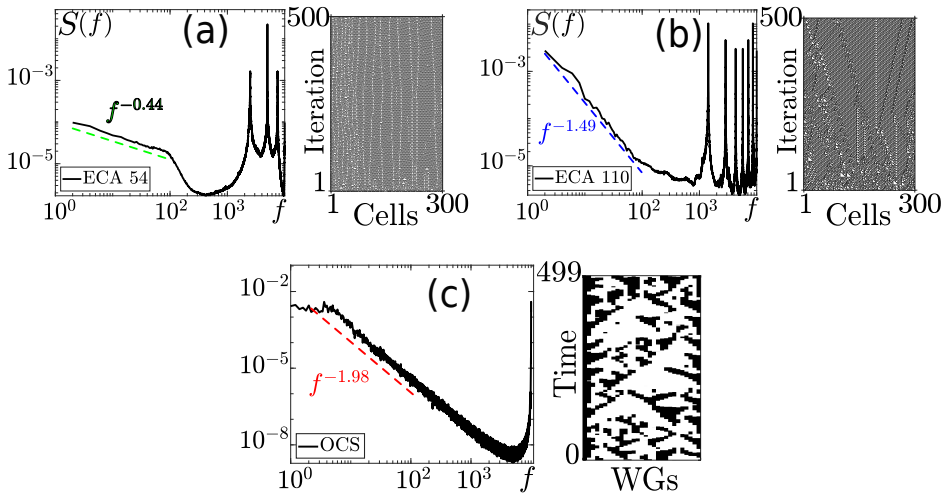

Fig. 8. (Color Online) Power spectral analysis of complex ECA rules and OCS. (a), (b) and (c): the left panels display the power spectrum $S(f)$ of the temporal behavior exhibited by complex ECA rules (54, 110) and OCS, respectively. The dashed lines represent the log-log fit of the power spectrum in the range of low frequencies $f = 2 - 10^2$ showing a power law with different slopes. the right panels display the typical space-time behaviors of complex ECA rules and OCS's incoherent domain.

Appendix A. Statistical measures

Here, we introduce briefly the statistical measures used in our investigation:

Appendix A.1. ApEn : Approximate Entropy

ApEn was proposed, to discern levels of regularity within real data without any knowledge about the source system [44]. It is robust to noise, which was a central limitation of the previous tools developed by the information theory [25]. Since then, ApEn was used to examine short experimental signals, especially, physiological and biological data sets [25].

In order to find the approximate entropy of a given time series of data $u = \{u(1), u(2), ..., u(N)\}$ of length N.

Firstly, we fix m (embedding dimension), a non-negative integer, so that blocks of $(N-m+1)$ vectors are formed $x(i) = \{u(i), u(i+1), ..., u(i+m-1)\}$ and $x(j) = \{u(j), u(j+1), ..., u(j+m-1)\}$, and we calculate the distance between them, given by :

$d[x(i), x(j)] = max_{k=1,2,...,m}(|u(i+k-1) - u(j+k-1)|)$.

Secondly, we calculate the value $C_i^m(r) =$ (number of $j <= N-m+1$ such that $d[x(i), x(j)] <= r)/(N-m+1)$ where r specifies the filtering level. Then, we compute $\Phi^m(r) = (N-m+1)^{-1} \sum_{i=1}^{N-m+1} log(C_i^m(r))$.

Finally, this statistic is defined as $ApEn(m, r, N) = \Phi^m(r) - \Phi^{m+1}(r)$.

Appendix A.2. SampEn : Sample Entropy

However, ApEn exhibits a major sensitivity to the input parameters: m (embedding dimension), r (filtering level) and L (Length of data). To avoid this chief drawback, the sample entropy SampEn [45] was introduced to overcome the dependence on the length of the time series and maintains the relative consistency [25, 45]. Theoretically, the main differences between ApEn and SampEn concern the calculation of probabilities. In fact, SampEn avoids the self-counting problem and adopts a different summation method of matches between template vectors.

To calculate SampEn of a time series data set:

First, we determine the sum number of *possible* vectors for each template vector and adding them by calculating the formula: $B^m(r) = [(N-m-1)(N-m)]^{-1} \sum_{i=1}^{N-m} \sum_{j=1, j\neq i}^{N-m}$[number of times that $d[|x_m(j) - x_m(i)|] < r$]. Likewise, we determine the sum number of *matches* for each template vector

and adding them by calculating the formula: $A^m(r) = [(N-m-1)(N-m)]^{-1} \sum_{i=1}^{N-m} \sum_{j=1,j\neq i}^{N-m}$[number of times that $d[|x_{m+1}(j) - x_{m+1}(i)|] < r$].

Finally, the value of SampEn is estimated by:

$SampEn(m, r, N) = -log[A^m(r)/B^m(r)]$.

Typical parameter combination ($r = 0.2 * std$, $m = 2$) [44, 45] was adjusted to perform our analysis either for $ApEn$ or $SampEn$.

Appendix A.3. LZ : Lempel-Ziv complexity

Another powerful tool that has proven its ability to measure and characterize randomness of dynamical models, is data compression. Roughly speaking, compression algorithms provide the length of the shortest form that can re-express the "essential" informations in a message. The LZ, one of the optimal compression algorithms, is used to estimate the entropy rate for an ergodic source, which is related to the asymptotic value of the the LZ growth rate reached in the limit of large string length ($L \gg 1$) [26, 43]. LZ was used for the classification of CA [43, 60], and nonlinear dynamical systems [61, 62].

Let (s) be a binary sequence of length N. The LZ complexity $C_{LZ}(s)$ of (s) is defined as the number of factors in its exhaustive history[26, 43]. As our binary strings have large length, we will consider the normalized measure of complexity given by: $LZ_{complexity} = C_{LZ}(s)/(N/log(N))$.

Appendix B. Data analysis method

Let us describe the outlines of our method. In fact, the spatiotemporal data of either ECA or OCS are binarized if needed and arranged of the form $\{x_t\}_{t=1}^T = \{x_1, x_2...., x_T\}$ where $x_t = (x_t(1), x_t(2)...., x_t(N))$ is the configuration at time t of a system of N sites. Each component $x_t(i)$ gives the state of the i-th site at time t. Next, we will consider only the mean value $\overline{x_t}$ at each time step. Following this scheme, we can build a time serie $\{S_t\}_{t=1}^T = \{S_1, S_1...., S_T\}$ where $S_t = \overline{x_t} \in$ [0,1], for every spatiotemporal diagram. It is on this averaged data that we apply the three statistical algorithms introduced above to quantify the randomness and to classify the different types of dynamics in ECA and OCS. It is necessary to emphasize that data must be of binary type for the estimation of the complexity LZ. Thus, for this later quantity the $\{S_t\}_{t=1}^T$ will be binarized following a threshold value given by its mean value.

Concerning ECA, simulations were performed for each rule, on 300 cell lattice over 3000 iterations where the first 500 transient states are discarded. Then the process is repeated for a 100 random initial conditions. Regarding OCS, the optical system is evolved for T units of time and its binarized intensity $||\psi_n(t)||^2$ is stored in an $N \times \frac{T}{dt}$ array (T=250, dt =0.0833), for different sizes of desynchronized region (δ_L). The binarization process was performed thanks to a cutoff value of intensity, allowing us to filter the OCS's spatiotemporal evolution to highlight the domains similar to those that arise in the ECA.

References

[1] G. Nicolis, Physics of far-from-equilibrium systems and self-organization, in: The new physics, 1993.

[2] J. Neumann, A. W. Burks, et al., Theory of self-reproducing automata, volume 1102024, University of Illinois press Urbana, 1966.

[3] C. G. Langton, Artificial life: An overview, Mit Press, 1997.

[4] L. Bunimovich, Coupled Map Lattices: at the Age of Maturity, Springer Berlin Heidelberg, Berlin, Heidelberg, 2005, pp. 9–32. URL: https://doi.org/10.1007/11360810_2. doi:10.1007/11360810_2.

[5] K. Kaneko, Spatiotemporal intermittency in coupled map lattices, Progress of Theoretical Physics 74 (1985) 1033–1044.

[6] Y. Kuramoto, D. Battogtokh, Coexistence of coherence and incoherence in nonlocally coupled phase oscillators., NONLINEAR PHENOMENA IN COMPLEX SYSTEMS 5 (2002) 380–385.

[7] D. M. Abrams, S. H. Strogatz, Chimera states for coupled oscillators, Phys. Rev. Lett. 93 (2004) 174102. URL: https://link.aps.org/doi/10.1103/PhysRevLett.93.174102. doi:10.1103/PhysRevLett.93.174102.

[8] G. C. Sethia, A. Sen, F. M. Atay, Clustered chimera states in delay-coupled oscillator systems, Phys. Rev. Lett. 100 (2008) 144102. URL: https://link.aps.org/doi/10.1103/PhysRevLett.100.144102. doi:10.1103/PhysRevLett.100.144102.

[9] O. E. Omel'chenko, Y. L. Maistrenko, P. A. Tass, Chimera states: The natural link between coherence and incoherence, Phys. Rev. Lett. 100 (2008) 044105. URL: https://link.aps.org/doi/10.1103/PhysRevLett.100.044105. doi:10.1103/PhysRevLett.100.044105.

[10] D. M. Abrams, R. Mirollo, S. H. Strogatz, D. A. Wiley, Solvable model for chimera states of coupled oscillators, Phys. Rev. Lett. 101 (2008) 084103. URL: https://link.aps.org/doi/10.1103/PhysRevLett.101.084103. doi:10.1103/PhysRevLett.101.084103.

[11] I. Omelchenko, O. E. Omel'chenko, P. Hövel, E. Schöll, When nonlocal coupling between oscillators becomes stronger: Patched synchrony or multichimera states, Phys. Rev. Lett. 110 (2013) 224101. URL: https://link.aps.org/doi/10.1103/PhysRevLett.110.224101. doi:10.1103/PhysRevLett.110.224101.

[12] O. E. Omel'chenko, Coherence–incoherence patterns in a ring of nonlocally coupled phase oscillators, Nonlinearity 26 (2013) 2469.

[13] A. M. Hagerstrom, T. E. Murphy, R. Roy, P. Hövel, I. Omelchenko, E. Schöll, Experimental observation of chimeras in coupled-map lattices, Nature Physics 8 (2012) 658–661.

[14] S. Nkomo, M. R. Tinsley, K. Showalter, Chimera states in populations of nonlocally coupled chemical oscillators, Phys. Rev. Lett. 110 (2013) 244102. URL: https://link.aps.org/doi/10.1103/PhysRevLett.110.244102. doi:10.1103/PhysRevLett.110.244102.

[15] F. Parastesh, S. Jafari, H. Azarnoush, Z. Shahriari, Z. Wang, S. Boccaletti, M. Perc, Chimeras, Physics Reports (2020).

[16] M. G. Clerc, S. Coulibaly, M. A. Ferré, M. A. García-Ñustes, R. G. Rojas, Chimera-type states induced by local coupling, Phys. Rev. E 93 (2016) 052204. URL: https://link.aps.org/doi/10.1103/PhysRevE.93.052204. doi:10.1103/PhysRevE.93.052204.

[17] M. G. Clerc, S. Coulibaly, M. Ferré, M. Tlidi, Two-dimensional optical chimera states in an array of coupled waveguide resonators, Chaos 30 (2020) 043107.

[18] Z. G. Nicolaou, H. Riecke, A. E. Motter, Chimera states in continuous media: Existence and distinctness, Phys. Rev. Lett. 119 (2017) 244101. URL: https://link.aps.org/doi/10.1103/PhysRevLett.119.244101. doi:10.1103/PhysRevLett.119.244101.

[19] A. Alvarez-Socorro, M. Clerc, M. Ferré, Wandering walk of chimera states in a continuous medium, Chaos, Solitons & Fractals 140 (2020) 110169.

[20] M. Clerc, M. Ferré, S. Coulibaly, R. Rojas, M. Tlidi, Chimera-like states in an array of coupled-waveguide resonators, Optics Letters 42 (2017) 2906–2909.

[21] H. Chaté, P. Manneville, Collective behaviors in spatially extended systems with local interactions and synchronous updating, Progress of theoretical physics 87 (1992) 1–60.

[22] S. Wolfram, Universality and complexity in cellular automata, Physica D: Nonlinear Phenomena 10 (1984) 1–35.

[23] S. Wolfram, Computation theory of cellular automata, Communications in mathematical physics 96 (1984) 15–57.

[24] C. Langton, Computation at the edge of chaos: Phase transition and emergent computation, Technical Report, Los Alamos National Lab., NM (USA), 1990.

[25] A. Delgado-Bonal, A. Marshak, Approximate entropy and sample entropy: A comprehensive tutorial, Entropy 21 (2019) 541.

[26] A. Lempel, J. Ziv, On the complexity of finite sequences, IEEE Transactions on information theory 22 (1976) 75–81.

[27] S. Wolfram, Statistical mechanics of cellular automata, Rev. Mod. Phys. 55 (1983) 601–644.

[28] K. Culik, S. Yu, Undecidability of ca classification schemes, Complex Systems 2 (1988) 177–190.

[29] W. Li, N. H. Packard, C. G. Langton, Transition phenomena in cellular automata rule space, Physica D: Nonlinear Phenomena 45 (1990) 77–94.

[30] A. Wuensche, Classifying cellular automata automatically: Finding gliders, filtering, and relating space-time patterns, attractor basins, and thez parameter, Complexity 4 (1999) 47–66. doi:10.1002/(SICI)1099-0526(199901/02)4:33.0.CO;2-V.

[31] G. Oliveira, P. De Oliveira, N. Omar, Definition and application of a five-parameter characterization of one-dimensional cellular automata rule space, Artificial Life 7 (2001) 277–301. doi:10.1162/106454601753238645.

[32] O. Egorov, U. Peschel, F. Lederer, Discrete quadratic cavity solitons, Physical Review E 71 (2005) 056612.

[33] O. Egorov, F. Lederer, Spontaneously walking discrete cavity solitons, Optics letters 38 (2013) 1010–1012.

[34] M. Clerc, S. Coulibaly, M. Ferré, M. Tlidi, Two-dimensional optical chimera states in an array of coupled waveguide resonators¡? a3b2 show [editpick]?¿, Chaos: An Interdisciplinary Journal of Nonlinear Science 30 (2020) 043107.

[35] J. P. Crutchfield, J. E. Hanson, Turbulent pattern bases for cellular automata, Physica. D, Nonlinear phenomena 69 (1993) 279–301.

[36] J. E. Hanson, J. P. Crutchfield, The attractor—basin portrait of a cellular automaton, Journal of statistical physics 66 (1992) 1415–1462.

[37] M. Mitchell, P. T. Hraber, J. P. Crutchfield, Revisiting the edge of chaos: Evolving cellular automata to perform computations, Complex Systems 7 (1993).

[38] J. T. Lizier, M. Prokopenko, A. Y. Zomaya, A framework for the local information dynamics of distributed computation in complex systems, in: Guided self-organization: inception, Springer, 2014, pp. 115–158.

[39] J. P. Crutchfield, K. Young, Inferring statistical complexity, Phys. Rev. Lett. 63 (1989) 105–108. doi:10.1103/PhysRevLett.63.105.

[40] J. P. Crutchfield, Between order and chaos, Nature Physics 8 (2012) 17–24.

[41] M. Martin, A. Plastino, O. Rosso, Generalized statistical complexity measures: Geometrical and analytical properties, Physica A: Statistical Mechanics and its Applications 369 (2006) 439–462.

[42] O. Rosso, H. Larrondo, M. Martin, A. Plastino, M. Fuentes, Distinguishing noise from chaos, Physical review letters 99 (2007) 154102.

[43] F. Kaspar, H. G. Schuster, Easily calculable measure for the complexity of spatiotemporal patterns, Phys. Rev. A 36 (1987) 842–848. URL: https://link.aps.org/doi/10.1103/PhysRevA.36.842. doi:10.1103/PhysRevA.36.842.

[44] S. M. Pincus, Approximate entropy as a measure of system complexity., Proceedings of the National Academy of Sciences 88 (1991) 2297–2301.

[45] J. S. Richman, J. R. Moorman, Physiological time-series analysis using approximate entropy and sample entropy, American Journal of Physiology-Heart and Circulatory Physiology 278 (2000) H2039–H2049.

[46] P. Grassberger, I. Procaccia, Characterization of strange attractors, Phys. Rev. Lett. 50 (1983) 346–349. doi:10.1103/PhysRevLett.50.346.

[47] M. Bauer, H. Heng, W. Martienssen, Characterization of spatiotemporal chaos from time series, Physical review letters 71 (1993) 521.

[48] W. Li, N. Packard, The structure of the elementary cellular automata rule space, Complex systems 4 (1990) 281–297.

[49] J. P. Crutchfield, K. Young, Computation at the onset of chaos, in: The Santa Fe Institute, Westview, Citeseer, 1988.

[50] N. H. Packard, Adaptation toward the edge of chaos, Dynamic patterns in complex systems 212 (1988) 293.

[51] H. Zenil, Compression-based investigation of the dynamical properties of cellular automata and other systems, Complex Systems 19 (2010) 1–28. doi:10.25088/ComplexSystems.19.1.1.

[52] H. Zenil, On the dynamic qualitative behavior of universal computation, Complex Systems 20 (2012) 265–278. doi:10.25088/ComplexSystems.20.3.265.

[53] W. Li, M. G. Nordahl, Transient behavior of cellular automaton rule 110, Physics Letters A 166 (1992) 335–339.

[54] S. Ninagawa, Power spectral analysis of elementary cellular automata, Complex Systems 17 (2008) 399.

[55] M. S. Keshner, 1/f noise, Proceedings of the IEEE 70 (1982) 212–218.

[56] Y. Pomeau, P. Manneville, Intermittent transition to turbulence in dissipative dynamical systems, Communications in Mathematical Physics 74 (1980) 189–197.

[57] M. Cook, Universality in elementary cellular automata, Complex systems 15 (2004) 1–40.

[58] S. Ninagawa, M. Yoneda, S. Hirose, 1f fluctuation in the "game of life", Physica D: Nonlinear Phenomena 118 (1998) 49–52.

[59] S. Ninagawa, Dynamics of universal computation and 1/f noise in elementary cellular automata, Chaos, Solitons & Fractals 70 (2015) 42–48.

[60] E. Estevez-Rams, R. Lora-Serrano, C. Nunes, B. Aragón-Fernández, Lempel-ziv complexity analysis of one dimensional cellular automata, Chaos: An Interdisciplinary Journal of Nonlinear Science 25 (2015) 123106.

[61] L. M. Alonso, Complex behavior in chains of nonlinear oscillators, Chaos: An Interdisciplinary Journal of Nonlinear Science 27 (2017) 063104.

[62] E. Estevez-Rams, D. Estevez-Moya, B. Aragón-Fernández, Phenomenology of coupled nonlinear oscillators, Chaos: An Interdisciplinary Journal of Nonlinear Science 28 (2018) 023110.

Graphical Abstract

The cellular automata inside optical chimera states

Marouane Ayyad, Saliya Coulibaly

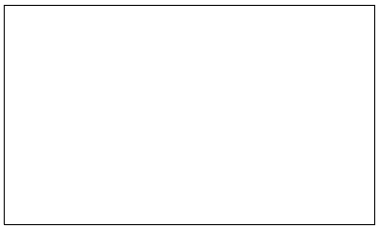

Highlights

The cellular automata inside optical chimera states

Marouane Ayyad, Saliya Coulibaly

- Research highlight 1
- Research highlight 2